

## Petrography and geochemistry of the Upper Cretaceous Gryphaea Limestones, Kallankurichi Formation, Ariyalur Group, Trichinopoly, Southern India: Implication for palaeoenvironment

M. Senthappan<sup>1, 2\*</sup>, V. Stephen Pitchaimani<sup>1</sup>, A.V. Udayanapillai<sup>3</sup>, Perumal Velmayil<sup>3</sup>, Bangarupriyanga Sundaram<sup>3</sup>, G. Ramalingam<sup>3</sup>, and John S. Armstrong-Altrin<sup>4, 5</sup>

<sup>1</sup> Department of Geology, V.O. Chidambaram College, Thoothukudi, Tamil Nadu, India

<sup>2</sup> Research Scholar, Affiliated to Manonmaniam Sundaranar University, Tirunelveli, Tamil Nadu

<sup>3</sup> Department of Geology & Quantum Material Research Laboratory, Department of Nano-Science & Technology, Alagappa University, Karaikudi, Tamil Nadu, India

<sup>4</sup> Unidad de Procesos Oceánicos y Costeros, Universidad Nacional Autónoma de México, Instituto de Ciencias del Mar y Limnología, Ciudad Universitaria, Mexico City, Mexico

<sup>5</sup> Department of Marine Sciences, Bharathidasan University, Tiruchirappalli, 620024, Tamil Nadu, India

### ABSTRACT

Sub-surface Kallankurichi gryphaea limestone formation is observed between Archaeal and Quaternary outcrops. Petrographic observation reveals that mega fossils are absent and it contains abundant skeletal fragments of pelecypods, gastropods, foraminifera, bryozoa, and symbiotic algae. X-ray diffraction (XRD) analyses reveal the mineralogical components of both carbonate and clay minerals. Carbonate minerals include calcite, siderite, witherite, malachite, smithsonite, and rhodochrosite. Clay minerals detected are kaolin, montmorillonite, and palygorskite. Major element composition represents predominance of CaO, SiO<sub>2</sub>, Al<sub>2</sub>O<sub>3</sub>, and Fe<sub>2</sub>O<sub>3</sub> oxides, while MgO, MnO, Na<sub>2</sub>O, K<sub>2</sub>O, TiO<sub>2</sub>, and P<sub>2</sub>O<sub>5</sub> oxides are depleted. Statistical analyses of correlation coefficient, principal component analysis, and cluster analysis represent the geochemical affinities and aerial distribution similarities among major elements. Palaeoclimate inferred through biotic proxies, major element geochemistry, and clay minerals represents arid and semi-arid climate.

**KEYWORD:** Kallankuruchi, Petrography, Major elements, XRD, Statistical analysis, Palaeoclimate,

### INTRODUCTION

Marine transgressions of the Indo-Pacific Sea during the Upper Cretaceous period have occupied the continental area centered on Ariyalur town, Tamil Nadu, India. These transgressions and regressions have caused for the formation of Uttatur, Trichinopoly, Ariyalur, and Niniyur groups of various sedimentary rocks and the preservation of many marine invertebrate groups of fossils (Krishnan, 1982). Hence, this area has been reported as a Cretaceous fossil heritage site with a field museum or Cretaceous Park of Tamil Nadu (Udayanapillai et al., 2020). Numerous authors have focused their research on the Upper Cretaceous Formation of Trichinopoly in various aspects (Blanford, 1862; Krishnan, 1982; Ramasamy et al, 1991; Ayyasamy et al, 1992; Banerji, 1996; Govindan et al, 1996; Madhavaraju et al, 1999, 2021; Sundaram Reddy A, N. et al, 2013; Goswamy et al, 2013; Babu, 2017; Nagendra and Nallappareddy, 2017; Nagendra et al., 2011, 2018; Ramkumar et al, 2018; Udayanapillai et al, 2020). Due to the widespread occurrence of Cretaceous limestone outcrops, many cement companies, like Dalmia, Chettinadu, Ramco, India cement, Gracim, Ultratech, Tancem, etc., have established their mining activities in and around the Ariyalur area.

Kallankurichi is one of the important limestone formations in the Ariyalur stage or group. It occurs as a S-type outcrop that extends from Periakuruchi village in the north and Pudupalayam village in the south. The northern band of the Kallankurichi limestone formation occurs as a surface outcrop, whereas the southern band occurs as a subsurface outcrop. A faulted structure can be observed in the 'S' type band of Kallankurichi limestone formation from the Pudupalayam mine area. There are several limestone mines in the Kallankurichi formation.

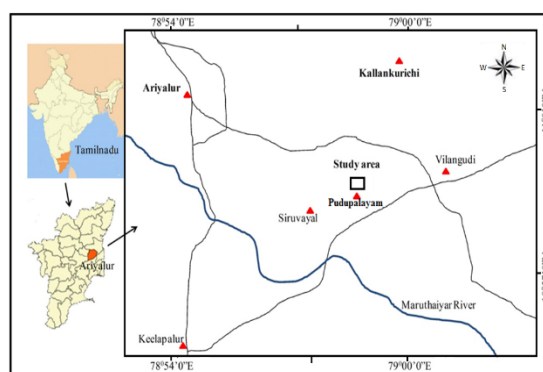


**Figure 1.** Location map of the study area

But still now no research has been carried out on the gryphaea limestone bed of the Pudupalayam Chettinadu mine, located in the terminal part of the Kallankurichi 'S' band limestone outcrop. In order to fulfil this gap, an attempt has been made to study the field observation, petrological observation, distribution of major elements, depositional environment and palaeoclimate

**STUDY AREA**

The area under investigation Pudupalayam Chettinadu limestone mine is located at 7 km from Ariyalur town, near the Ariyalur-Tiruchirappalli state highway. Proposed mine area lies at the latitude 11.10072° N and longitude 79.15059° E. The area has been well connected with Tanjore, Trichy, and Ariyalur town by state highway road networks. Physiography of the area is almost flat with an elevation range of 62 m above M.S.L. Coleroon and Maruthaiyar rivers are running from the southern side to the study area (Fig. 1)

**GEOLOGICAL SETTING**

The geological outcrop map of Ariyalur district (Nagendra et al., 2011) is shown in (Fig. 2).

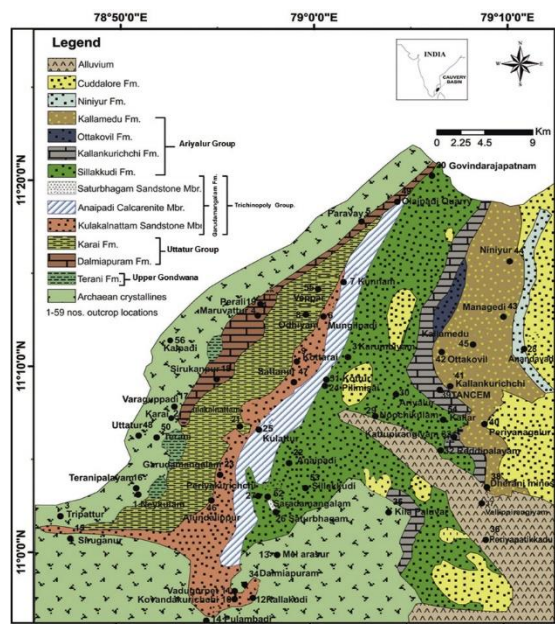


Figure 2. The Geological map of the Ariyalur district (modified after Nagendra et al., 2011).

Post-Archaean/Archaean hard basement rocks consist of granite, granitic gneiss, and charnockite. The basement rocks are unconformably overlain either by the Upper Gondwana Formation or directly rest on Upper Cretaceous group of rocks which consist of Uttatur, Trichinopoly, Ariyalur, and Niniyur stages (Krishnan, 1982). Later, over all established entire sequential stratigraphy of Upper Cretaceous rocks of Trichinopoly have been published (Sundaram et al., 2001; Nagendra et al.,

2002; Udayanapillai et al., 2020) (Table 1). Ariyalur stage consists of several formations. The lowermost formation is Sillakudi sandstone. It is overlain by the Kallankurichi limestone formation with an unconformity and is followed by

Era	Stage	Formation	Lithology	
Tertiary		Cuddalore	Red Sandstone	
Upper Cretaceous	Niniyur	Nanniyur	Arenaceous Limestone	
		Athanakuruchi	Limestone	
	Ariyalur	Sendurai	Arenaceous Limestone	
		Ottakovil	Arenaceous Limestone	
		Kallamedu	Sandstone	
		Kallankurichi		Arenaceous Limestone
				Gryphaea Limestone
				Arenaceous Limestone
				Ferruginous Gryphaea Limestone
			Conglomerate	
	Sillakudi	Sandstone		
	Trichinopoly	Kunnam	Shale	
		Paravai	Arenaceous limestone	
		Sathanur	Shale	
		Kollakanattham	Clay, Arenaceous Sandstone	
Anaipadi		Red Sandstone		
Garudamangalam		Argillaceous limestone		
Uttatur		Maruvathur	Clay and shale	
	Karai	Shale		
	Dalmiapuram formation		Marl bedded argillaceous l.stone	
			Bedded limestone	
			Coralline algal limestone	
Shale	Calcareous Grey Shale			
Conglomerate_unconformity				
Upper Gondwana		Therani	Variegated clay	
			Purple sandstone	
Conglomerate-Unconformity				
Archean		Charnockite and granitic gneiss		



**Figure 3.** Field photograph of Pudupalayam mine section

Kallamedu, Ottakovil, and Sendurai calcareous sandstone formations (**Table 2**). Kallankurichi limestone outcrop is bordered by the formation of the Sillakudi sandstone outcrop in the west, Kallamedu, Ottakovil and Sendurai outcrops in the eastern side, and Archaean outcrop in the south. The study area Pudupalayam Chettinadu mine is located at the southern terminal part of the ‘S’ band’ type Kallankurichi limestone outcrop.

**METHODOLOGY**

Intensive fieldwork was undertaken in January 2020 to investigate the nature of the Pudupalayam Chettinadu mines. Nature of the Gryphaea limestone outcrop and its other lithological associations were carefully studied with available literatures concerning the geology and geochemistry of gryphaea limestone. Gryphaea limestone is the typical characteristic bed in the Kallankurichi formation (Ramasamy et al., 2012; Nagendra et al., 2018; Ramkumar et al., 2020). Ten gryphaea limestone samples were collected at the interval of 1 foot between the occurrence of limestone profile (5-10 m) in the vertical mine profile section. Thickness of beds and intervals were measured. Then, the collected samples were properly packed and labelled with GPS co-ordination. While collecting samples, megascopic characters of limestone samples were also observed in the field. Then limestones thin sections were prepared at Suchitra polishing unit, in Chennai. In addition, limestone samples were analysed for major oxides through an XRF instrument (X-Ray Fluorescence spectroscopy) at the laboratory of the National Centre for Earth Science Studies (NCESS), Thiruvananthapuram. Three representative samples were selected for clay

mineral analysis by an X-ray Diffraction (XRD) method at University Scientific Instrumentation Centre (USIC), Department of Physics, Alagappa University, Karaikudi. Photomicrographs of thin sections were taken from the laboratory at Department of Geology, University of Madras, Chennai.

**FIELD OBSERVATION**

Entire mine section shows Archaean, Upper Cretaceous, Sub-Recent and Recent outcrops from the bottom to the top of the mine. Lower-most Archaean granitic gneiss outcrop can be observed at the depth of 30 m in the mine area. Kallankurichi limestone of Ariyalur stage unconformably rest on same stage Cretaceous bed of the Sillakudi sandstone formation which occurs at a depth from 11m to 26 m. A conglomerate bed of 0.5m thickness separates the Sillakudi sandstone formation and Kallankurichi limestone formation (Table2). Gryphaea limestone bed occurs between 4.5 metres and 9.5 metres depth with a thickness of 5 m. Gryphaea limestone bed is followed by marl, chert, calcrete and black soil of Quaternary age.

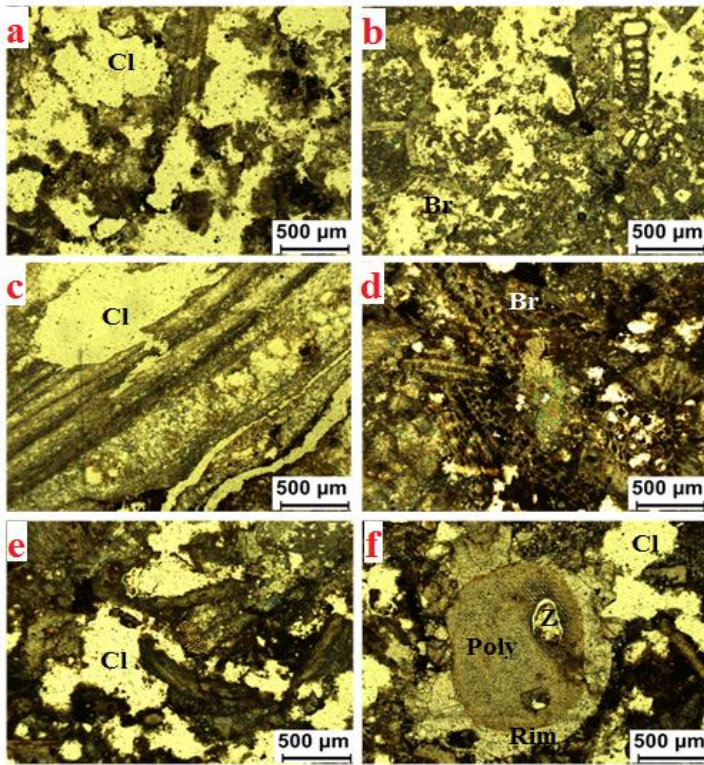
Gryphaea limestone collected from the Pudupalayam mine show grey, pale yellow and

Table 2. Stratigraphy of the Ariyalur stage at Pudupalayam Chettinadu mine

Age	Stage	Formation	Lithology	Depth from Top in metres	Thickness in metres
Recent			Top soil/ Red soil/ Black soil	0 to 0.5	0.5
Holocene – Pleistocene (or) Sub - Recent			Calcrete	0.5 to 1.5	1
Upper Cretaceous	Ariyalur	Kallankurichi	Arenaceous Limestone	1.5 to 4.5	3
			Gryphaea Limestone	4.5 to 9.5	5 (study area)
			Arenaceous Limestone	9.5 to 12.5	3
			Ferruginous Gryphaea Limestone	12.5 to 22.5	10
			Conglomerate - Unconformity	22.5 to 23	0.5
	Sillakudi	Sillakudi sandstone formation	Below 23	8	

ferruginous colour without mega fossils. It is highly compacted and indurated. Compaction and indurations are mainly made by CaCO<sub>3</sub> mineral grains with a very few detrital grains. Entire litho-profile section of the Pudupalayam Chettinadu mine section is shown in the field photographs and table (**Fig. 3; Table 2**).

**PETROLOGICAL OBSERVATION**



**Figure 4 (a-f).** Photomicrographs of gryphaea limestone of pudupalayam Chettinadu mine. a) Photomicrograph shows equal preservation of Bryozoa and more white lime mud clast in the ferruginous micritic calcite matrix. b) Photomicrograph shows preservation of uniserial chambered foraminifera *Nodosaria* with algal mats, gryphaea group shell fragments and also possesses more white lime mud clast preservation in the ferruginous micritic calcite matrix. c) Photomicrograph shows parallel algal mats preservation with micritic calcite and lime mud clast. d) Photomicrograph shows full of bryozoan colony within ferruginous micritic calcite matrix. e) Photomicrograph shows pelecypod shell fragments, Polyphora-Bryozoa and lime mud clast preservation in the micritic calcite matrix. f) Photomicrograph shows a large Polyphora-Bryozoa with zoecia rimmed by micritic calcite and lime mud clast in the ferruginous micritic calcite matrix.

Petrographically Maastrichtian limestones were classified as packstone/grainstone facies or as wackestone and mudstone facies (Nagendra et al., 2011). Classification of limestone has been proposed by Dunham (1962) and Folk (1968). Dunham has classified the limestone as mudstone, wackestone, and packstone, based on the fabric of the rock. Folk (1968) has classified the limestone as autochthonous and allochthonous limestones, based on grain and cement types. A revised classification was proposed by Wright (1997), based on the diagenetic pattern. Gryphaea limestone beds of Pudupalayam is a mud based biogenic limestone, as per the classification of Wright (1997). Despite large mega-fossils are being absent in the limestone, it contains numerous desmodont gryphaea group shell fragments of pelecypods, gastropods, micro-faunal distribution of foraminifera, bryozoa and algal mats. These

biogenic materials are preserved in the ferruginous or calcified micritic or micro-sparitic calcite matrix. Rich iron content in the biogenic limestone indicates shallow and high energy conditions of the sea (Nagendra et al., 2011). Such similar condition may be existed in the study area. Shell fragments and algal mats have caused for the formation of ferruginous micritic calcite matrix, during diagenesis and lithification. The uniserial foraminifera *Nodosaria* with lime mud clast preservation was also observed in the ferruginous micritic calcite matrix. Some thin section photomicrograph shows parallel algal mats preservation with micritic calcite and lime mud clast. In general, carbonate microfacies of Pudupalayam gryphaea limestone indicates that these limestones were formed in a continental marginal platform. Such similar reports have already been reported in the other areas of the Kallankurichi formation (Nagendra et al., 2011). Photomicrographs of gryphaea limestone samples of the Pudupalayam mine are given in (Fig. 4 a-f).

#### X-RAY DIFFRACTION ANALYSIS

Numerous researchers have applied XRD technique for the identification of minerals in sediments and sedimentary rocks (Carrol 1970; Deer et al., 1979; Mitra 1989; Kile and Dennis, 2000; Jimenez-Espinosa and Jimenez-Millan, 2003; Udayanapillai et al., 2015; Perumal and Udayanapillai, 2020; Armstrong-Altrin et al., 2021, 2022; Ramos-Vázquez et al., 2022; Udayanapillai et al., 2022). Based on high angle XRD mineral analysis (2 theta 0-80 degree), d spacing values and their relative intensities of powdered gryphaea limestone samples reveals the presence of

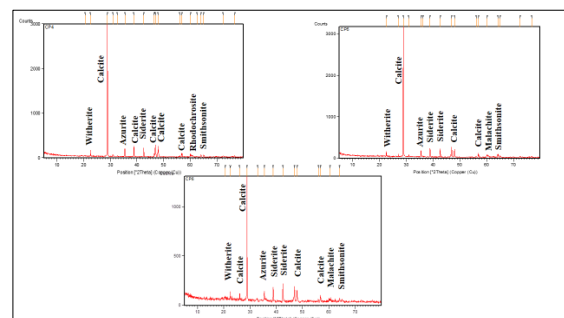


**Figure 5a.** XRD diffractogram pattern of the gryphaea limestone samples (all minerals) of Pudupalayam Chettinadu mine

minerals of calcite, siderite, witherite, malachite, smithsonite, azurite and rhodochrosite. Low angle XRD Clay mineralogy (2 theta 0-30 degree)

analysis of powdered gryphaea limestone samples indicates the presence of clay minerals of kaolin, montmorillonite, and palygorskite. Mineralogy of gryphaea limestone with d spacing values and their intensities are given in **Figure 5 a-b** and **Table 3**.

**Table 3. The clay and general mineralogy of Limestone samples of Chettinadu mine**

S. no.	Minerals	D-Space values A°	Name of the mineral	Chemical Composition
1	Clay minerals	3.95	Kaolinite	Al <sub>4</sub> [Si <sub>4</sub> O <sub>10</sub> ] (OH) <sub>3</sub>
2		15.26	Montmorillonite	Al <sub>2</sub> [Si <sub>4</sub> O <sub>10</sub> ] (OH) <sub>2</sub> .nH <sub>2</sub> O
3		3.42	Kaolinite	Al <sub>4</sub> [Si <sub>4</sub> O <sub>10</sub> ] (OH) <sub>3</sub>
4		4.31	Palygorskite	Mg <sub>3</sub> H <sub>2</sub> Si <sub>8</sub> O <sub>22</sub> (H <sub>2</sub> O).2H <sub>2</sub> O
5	Other minerals	3.09	Calcite	CaCO <sub>3</sub>
6		2.53	Azurite	Cu <sub>3</sub> (CO <sub>3</sub> ) <sub>2</sub> (OH) <sub>2</sub>
7		2.12	Siderite	FeCO <sub>3</sub>
8		1.89	Calcite	CaCO <sub>3</sub>
9		1.93	Calcite	CaCO <sub>3</sub>
10		1.62	Calcite	CaCO <sub>3</sub>
11		1.53	Rhodochrosite	MnCO <sub>3</sub>
12		1.45	Smithsonite	ZnCO <sub>3</sub>
13		1.43	Smithsonite	ZnCO <sub>3</sub>
14		3.95	Witherite	BaCO <sub>3</sub>
15		2.31	Siderite	FeCO <sub>3</sub>
16		3.43	Calcite	CaCO <sub>3</sub>
17		1.93	Calcite	CaCO <sub>3</sub>
18	1.54	Malachite	Cu <sub>2</sub> CO <sub>3</sub> (OH) <sub>2</sub>	

**GEOCHEMICAL OBSERVATION**

Major element concentrations of gryphaea limestones from the Pudupalayam mine, shows a more or less similar distribution trend (**Table 4; Fig. 6**). Distribution of CaO, SiO<sub>2</sub>, Al<sub>2</sub>O<sub>3</sub>, Fe<sub>2</sub>O<sub>3</sub>, and LOI shows higher concentration, which is above 1%, whereas other major oxides, viz. MgO,

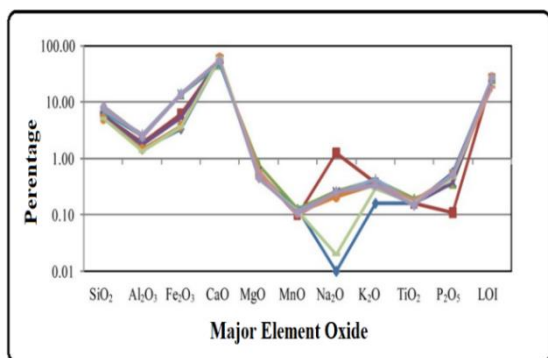


**Figure 6.** Comparison of Major elements distribution of Gryphaea Limestone samples of Chettinadu Pudupalayam mine

MnO, Na<sub>2</sub>O, K<sub>2</sub>O, TiO<sub>2</sub>, and P<sub>2</sub>O<sub>5</sub> are below 1%. Average distributions of major element concentrations of samples are taken into

consideration for geochemical discussion, as they show similar distribution trend.

Average SiO<sub>2</sub> concentration of gryphaea limestone is 6.56, whereas the average concentration of Al<sub>2</sub>O<sub>3</sub> is 2.05. Al<sub>2</sub>O<sub>3</sub> concentration may generally be attributed to a good mixture of transported flux and limited SiO<sub>2</sub> may be due to less concentration of detrital unaltered quartz and feldspar contents (Ramasamy et al., 2007; Cox et al., 1995; Udayanapillai and Ganesamurthy, 2013; Ekoa Bessa et al., 2021a,b; Madhavaraju et al., 2021; Sopia et al., 2023). Gryphaea limestone represents less SiO<sub>2</sub>/Al<sub>2</sub>O<sub>3</sub> ratio (3.22), which indicates that the detrital concentration of quartz and feldspar is limited in the samples. Al<sub>2</sub>O<sub>3</sub> is used as a proxy for clay content in limestone. K<sub>2</sub>O/Al<sub>2</sub>O<sub>3</sub> ratio of sediment can be used as an indicator of the original composition (Udayanapillai and Ganesamurthy, 2013; Anaya-Gregorio et al., 2018; Tawfik et al., 2018). K<sub>2</sub>O/Al<sub>2</sub>O<sub>3</sub> ratio of clay minerals and feldspar are different (0.00 to 0.3; 0.3 to 0.9) respectively (Cox et al., 1995;). Average K<sub>2</sub>O/Al<sub>2</sub>O<sub>3</sub> ratio in limestones is 0.16, which is close to the limit of the clay mineral range. It indicates that kaolinite,

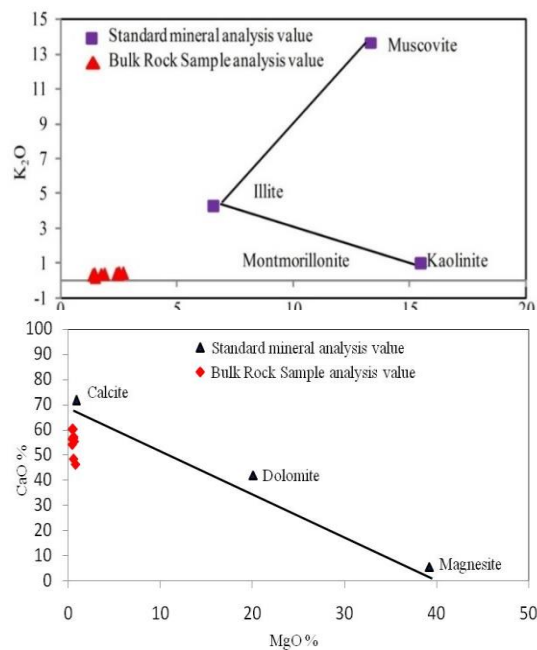


**Figure 7(a).** Bivariate plot K<sub>2</sub>O vs Al<sub>2</sub>O<sub>3</sub> in the gryphaea limestone samples (after Mc Queen 2006, modified with the standard analytical result of minerals analysis from Deer et al., 1978 and Udayanapillai et al., 2014), **(b).** Bivariate plot of CaO Vs MgO (after Queen, 2006, modified with the standard analytical result of minerals analysis from Deer et al., 1978 and Udayanapillai et al., 2014)

montmorillonite, and illite may be the dominant clay minerals in the limestone samples (**Fig. 7a**).

Average CaO contents shows 55.58%, whereas MgO content represents 0.54%. Lesser

Table 4: Data of major element concentrations (in wt. %) of Chettinadu Gryphaea limestones, Puthupalayam  
LOI = Loss of Ignition

Major element	S-1	S-2	S-3	S-4	S-5	S-6	S-7	S-8	S-9	S-10	Average
SiO <sub>2</sub>	5.13	5.76	8.4	5.6	6.7	5.12	7.3	8.2	5.15	8.3	6.56
Al <sub>2</sub> O <sub>3</sub>	1.5	1.89	2.51	1.76	2.46	1.48	2.7	2.5	1.39	2.4	2.05
Fe <sub>2</sub> O <sub>3</sub>	3.37	6.19	14.1	5.41	13.9	3.74	14.12	13.8	3.72	13.7	9.2
CaO	60.3	57.4	46.5	56.7	48.4	60.21	56.3	55.4	60.34	54.3	55.58
MgO	0.47	0.54	0.76	0.6	0.54	0.53	0.44	0.62	0.46	0.46	0.54
MnO	0.13	0.1	0.13	0.11	0.12	0.11	0.12	0.1	0.12	0.11	0.11
Na <sub>2</sub> O	0.01	1.26	0.27	0.26	0.23	0.21	0.25	0.26	0.02	0.26	0.3
K <sub>2</sub> O	0.16	0.37	0.42	0.38	0.36	0.35	0.43	0.35	0.3	0.34	0.34
TiO <sub>2</sub>	0.16	0.16	0.2	0.16	0.17	0.16	0.17	0.18	0.16	0.15	0.16
P <sub>2</sub> O <sub>5</sub>	0.56	0.11	0.36	0.38	0.53	0.52	0.53	0.49	0.48	0.53	0.44
LOI	27.44	26.9	25.99	26.9	26.84	27.32	18.42	18.9	27.3	27.3	25.33

Table 5. Multiple correlation of major element concentrations

Oxides	SiO <sub>2</sub>	Al <sub>2</sub> O <sub>3</sub>	Fe <sub>2</sub> O <sub>3</sub>	CaO	MgO	MnO	Na <sub>2</sub> O	K <sub>2</sub> O	TiO <sub>2</sub>	P <sub>2</sub> O <sub>5</sub>	LOI
SiO <sub>2</sub>	0.00										
Al <sub>2</sub> O <sub>3</sub>	0.90	0.00									
Fe <sub>2</sub> O <sub>3</sub>	0.93	0.98	0.00								
CaO	-0.71	-0.74	-0.78	0.00							
MgO	0.40	0.28	0.29	-0.63	0.00						
MnO	-0.04	-0.02	0.01	-0.26	0.03	0.00					
Na <sub>2</sub> O	-0.01	0.09	-0.01	-0.04	0.13	-0.58	0.00				
K <sub>2</sub> O	0.50	0.61	0.57	-0.52	0.41	-0.27	0.34	0.00			
TiO <sub>2</sub>	0.55	0.53	0.53	-0.68	0.81	0.33	-0.07	0.42	0.00		
P <sub>2</sub> O <sub>5</sub>	0.09	0.07	0.16	0.08	-0.38	0.40	-0.89	-0.34	-0.11	0.00	
LOI	-0.50	-0.63	-0.55	0.07	-0.02	0.20	0.04	-0.39	-0.39	-0.19	0.00

concentration of MgO content indicates the absence of dolomite mineral content in the limestone samples. In general, CaO/MgO ratio in dolomite mineral 40:20 (Deer et al., 1978). Average CaO/MgO ratio in limestones of this study is 102.93. A higher value of the above ratio indicates that the samples are high-grade limestone and possess more percentage of calcite mineral than the other carbonate minerals (**Fig. 7b**). Bulk rock containing more calcite mineral may derived from shell fragments of pelecypod, gastropod, foraminifera, bryozoa, etc. CaO shows negative correlation with SiO<sub>2</sub> and Al<sub>2</sub>O<sub>3</sub>, which indicates the effect of clastic input and detrital dilution of carbonate, during deposition (Ali and Wagreich, 2017). Fe<sub>2</sub>O<sub>3</sub>/Al<sub>2</sub>O<sub>3</sub> ratio of limestones show a high ratio (4.16), which may be due to the preservation of sesquioxide (Fe<sub>2</sub>O<sub>3</sub>Al<sub>2</sub>O<sub>3</sub>), clay mineral derived either from lithogenic sources or from the source of burial digenesis of Cretaceous marine invertebrate shells, due to marine transgression and regression. MnO and Na<sub>2</sub>O in limestones are low, due to less amount of lithogenic concentration.

Titanium oxide is mainly concentrated from phyllosilicates (Ramasamy et al., 2007; Udayanapillai and Ganesamoorthy, 2013). Titanium is relatively immobile (McLennan et al., 1993; Ramasamy et al., 2007). The samples of the area show lower TiO<sub>2</sub> (0.16%), which indicates lesser concentration of Titanium bearing minerals in limestones. P<sub>2</sub>O<sub>5</sub> content shows an average concentration of 0.44%. Low P<sub>2</sub>O<sub>5</sub> may be due to the presence of a lesser amount of accessory mineral phases, such as apatite and monazite minerals (Armstrong-Altrin et al., 2018; Chougong et al., 2021).

#### GEO-STATISTICAL EVALUATION

Advanced statistics of Multiple correlations, Principal Component Analysis, and Cluster Analysis are carried out for the major element concentrations of the gryphaea limestone of the Puthupalayam Chettinadu mine. Geostatistical software "PAST" is used for the statistical analysis.

**MULTIPLE CORRELATIONS**

It is a measure of the degree of dependency between the variable with one. Many researchers have utilized this technique in various studies (Srinivasamoorthy et al., 2010; Kaliammal and Udayanapillai, 2018; Udayanapillai et al., 2022). There are very limited reports have been published on applying these techniques in shell limestones. Multiple correlations of major elements of gryphaea limestone samples of Pudupalayam mine are given in **Table 5**. Multiple diagonally symmetrical linear correlation coefficient factor numbers of eleven parameters are given in bold letters. Correlation matrix represents that CaO makes negative relations with SiO<sub>2</sub>, Al<sub>2</sub>O<sub>3</sub>, Fe<sub>2</sub>O<sub>3</sub>, MgO, MnO, Na<sub>2</sub>O, K<sub>2</sub>O, and TiO<sub>2</sub> and positive relations with P<sub>2</sub>O<sub>5</sub>. Further, this relation indicates that CaO may be derived from the burial diagenetic process of Cretaceous marine invertebrates of pelecypods, gastropods, foraminifera, bryozoa, coralline algae, and brachiopod, etc. Other oxides might have been derived from continental lithogenic sources. CaO and P<sub>2</sub>O<sub>5</sub> show positive correlations, which indicates both elements were derived from a similar source.

**PRINCIPAL COMPONENT ANALYSIS**

It is a statistical procedure in which larger data can be changed into visualized one and analysed by a set of summary indices. It finds the direction of the maximal variance of data. It examines the magnitude and direction of coefficients for the original variables. Many researchers have applied Principal Component Analysis (PCA) in various geological studies (Srivastava et al., 1998; Sridhar et al., 2014; Usman et al., 2014; Udayanapillai and Kaliammal, 2016; Kuttalingam et al., 2018; Armstrong-Altrin, 2020; Ramos Vázquez and Armstrong-Altrin, 2019, 2021; Udayanapillai et al., 2022; Botello et al., 2023). PCA is regulated by linearity, the significance of mean, covariance, and orthogonal axis fitting of data of components (Udayanapillai et al., 2022). PCA data reveal its Eigen value, Percentage of Variance, Cumulative Variance, and the selected PCA components. Eigen value 1 is considered for the selection of PCA components (**Table 6a and b**). The canonical representation diagrams of the PCA components are given in **Figure 8**.

Four PCA components reveal 90.17% of Cumulative

Variance. Each PCA component is associated with

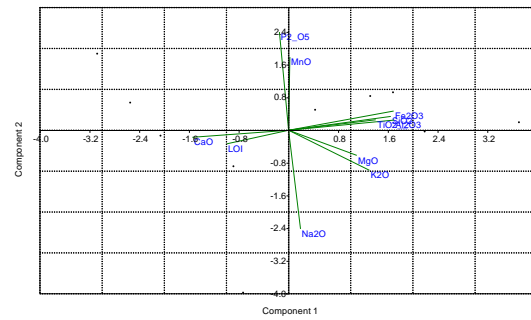


**Figure 8.** Canonical representation diagram of the PCA analysis.

certain major oxides and is provided as follows.

- I Component - SiO<sub>2</sub> + Al<sub>2</sub>O<sub>3</sub> + Fe<sub>2</sub>O<sub>3</sub> + CaO + K<sub>2</sub>O + TiO<sub>2</sub> -- 45.25% Variance
- II Component - MnO+Na<sub>2</sub>O+P<sub>2</sub>O<sub>5</sub> -- 22.61% Variance
- III Component - MgO +TiO<sub>2</sub> --15.20% Variance
- IV Component - LOI -- 7.12% of Variance.

Table 6a. Principal Component Analysis of geochemical data, LOI = Loss of Ignition

PC	Eigenvalue	% variance	Cumulative variance	Components
1	4.97798	45.254	45.254	SiO <sub>2</sub> + Al <sub>2</sub> O <sub>3</sub> + Fe <sub>2</sub> O <sub>3</sub> + CaO+K <sub>2</sub> O
2	2.48738	22.613	67.87	MnO+ Na <sub>2</sub> O+ P <sub>2</sub> O <sub>5</sub>
3	1.67184	15.199	83.06	MgO+ TiO <sub>2</sub>
4	0.783383	7.1217	90.19	LOI
5	0.46488	4.2262		
6	0.430687	3.9153		
7	0.121338	1.1031		
8	0.037837	0.34397		
9	0.024683	0.22439		

First component keeps the position of the highest amount of variation in the sample, whereas the fourth component has a lesser significance of variation. PCA component loading variations are

Table 6b. Component loading Scores  
LOI = Loss of Ignition

0	Axis 1	Axis 2	Axis 3	Axis 4	Axis 5	Axis 6	Axis 7	Axis 8	Axis 9	Axis 10	Axis 11
SiO <sub>2</sub>	0.90	0.13	-0.18	0.14	-0.18	-0.18	0.25	0.03	0.00	0.00	0.00
Al <sub>2</sub> O <sub>3</sub>	0.93	0.10	-0.29	0.16	0.10	-0.07	-0.05	-0.06	0.05	0.00	0.00
Fe <sub>2</sub> O <sub>3</sub>	0.92	0.18	-0.25	0.22	0.00	-0.06	-0.03	0.02	-0.03	0.00	0.00
CaO	-0.84	-0.07	-0.36	-0.34	0.03	-0.03	0.16	0.03	0.04	0.00	0.00
MgO	0.60	-0.24	0.64	-0.28	-0.30	-0.02	0.00	-0.06	0.07	0.00	0.00
MnO	0.01	0.69	0.55	0.10	0.45	0.00	0.09	-0.02	0.04	0.00	0.00
Na <sub>2</sub> O	0.10	-0.93	-0.08	0.15	0.21	-0.18	-0.06	0.07	0.07	0.00	0.00
K <sub>2</sub> O	0.71	-0.38	-0.11	-0.04	0.09	0.57	0.07	0.02	0.01	0.00	0.00
TiO <sub>2</sub>	0.76	0.10	0.47	-0.39	0.09	-0.09	-0.04	0.11	-0.04	0.00	0.00
P <sub>2</sub> O <sub>5</sub>	-0.08	0.93	-0.26	0.00	-0.18	0.10	-0.10	0.08	0.08	0.00	0.00
LOI	-0.54	-0.13	0.59	0.55	-0.19	0.09	0.04	0.06	0.00	0.00	0.00

gradually reduced from the first component to the fourth component.

### CLUSTER ANALYSIS

It is a statistical method that is used to group similar objects into respective categories. It can also be referred to as segmentation analysis. It confirms homogeneous and heterogeneous groups on a definite set of variables. Relative distance or proximity is taken into consideration for groups and these groups are called clusters. Cluster analysis represents a direct relationship between the variables, which function based on correlation matrices and the arithmetic average of the correlation coefficient (Davis, 1973, Harper, 1999). Numerous researchers have applied cluster analysis for various geological studies (Srivastava et al, 1998; Praus, 2007; Udayanapillai and Kaliammal, 2016; Kuttalingam et al., 2018; Udayanapillai et al., 2022).

Cluster analysis is applied here for two purposes, such as

- To interpret the ionic similarity between major element oxide parameters in the samples.
- Similar aerial grouping similarity concentration of cluster of the profile samples. Dendrogram of Paired group cluster method and Wards minimum variable cluster methods are used for finding out ionic similarity identification and finding out the relative distance of similarity of the profile samples (Fig. 9 a and b).

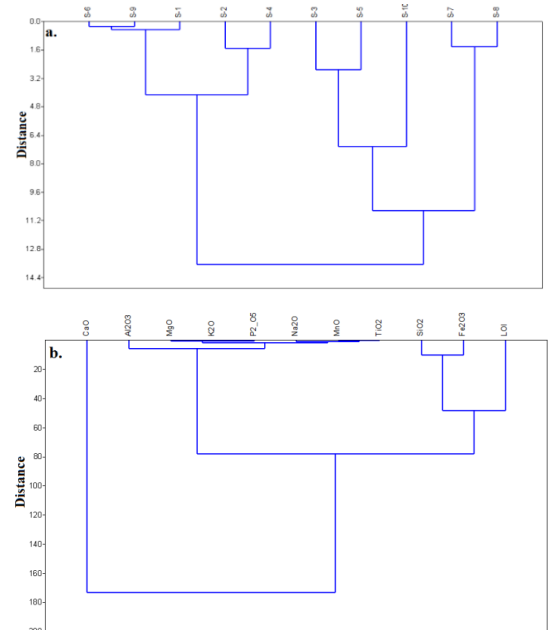


**Figure 9(a).** Ward method cluster analysis for aerial grouping of samples, **(b).** Paired group cluster methods of ionic similarities in the study area.

There are two paired groups of ionic clusters of major oxide are interpreted, which are as follows.

S.No	Cluster Component	Similarity of Correlation Coefficient
1	LOI+P <sub>2</sub> O <sub>5</sub> -SiO <sub>2</sub>	50
2	TiO <sub>2</sub> +MnO+Na <sub>2</sub> O+P <sub>2</sub> O <sub>5</sub> +K <sub>2</sub> O+MgO+Al <sub>2</sub> O <sub>3</sub>	10

The above two ionic clusters represent an average relative similarity value of 170.

There are two aerial grouping clusters by the Wards method or Euclidean method. They represent as follows:

- Cluster – S<sub>8</sub> - S<sub>7</sub> + S<sub>10</sub> + S<sub>5</sub> - S<sub>3</sub> -- Relative distance --11.2
- Cluster – S<sub>4</sub> - S<sub>2</sub> + S<sub>1</sub> + S<sub>9</sub> - S<sub>6</sub> -- Relative distance -- 4.0

Above two aerial groups form an average relative distance of 13.6.

Thus, the relativity of major oxide parameters and the profile samples inter-relationship quality is interpreted by advanced geostatistical techniques, such as Multiple Correlations, Principal component analysis, and Cluster analysis.

### PALAEOCLIMATE

Changes in climate through geological time are termed as palaeoclimate. A proxy or many numbers of proxies establish the palaeoclimate of an area. Stable isotope geochemical characters, tree rings analysis, pollen analysis, lake varves, biota or fossil evidence, ice cores, geological setting, historical documents, geochemical elements, clay minerals, etc. are some of the important proxies which represent palaeoclimate. Despite many proxies being used in the palaeoclimate studies, the palaeoclimate of the gryphaea limestone deposit of the Pudupalayam Chettinadu mine has been mainly interpreted by the proxies of biota, major element geochemistry, and clay minerals.

### BIOTA PROXIES

Thin section photomicrograph reveals the presence of microfossil bryozoa, foraminifera, algal mats, pelecypod, and gastropod shell fragments. Bryozoans are chiefly identified by using skeletal characteristics, like spines, surface structure, pores, and shape and size of the colonies. Bryozoa occur both in shallow and moderately deep-water deposits (Shrock and Twenhofel, 2005). Cheilostomata, Cyclostomata, Ctenostomata Bryozoans were almost equally numerous in the late Cretaceous (David Jablonski et al., 1997; Lidgard et al., 2016). Bryozoa are dominant contributor of CaO in temperate water in marine carbonate deposits (Clark and Ligards, 2000). The presence of algal mats indicates that symbiotic algae live in shallow tropical water. Pelecypod and gastropod shell fragments along with microfossils,

foraminifera and bryozoa are preserved in the shallow continental shelf marine platform of limestone deposits in the tropical climate. Since these limestone deposits are subjected to tectonic disturbances, mega fossils are damaged into small shell fragments.

### GEOCHEMICAL PROXIES

Geomorphological, sedimentological, and biological factors reflect climate changes. Evaporite mineral and major element geochemistry are the two important proxies used for palaeoclimate investigation in the evaporite deposit of Tunisia and Rajasthan (Sinha et al., 2006; Smykatzkloss and Roy, 2010) and the Pandalkudi calcrete profile (Udayanapillai et al., 2021). Calcite, dolomite, halite, anhydrite, and gypsum are important evaporite minerals that represent proxies for the arid environment. Calcite and other carbonate minerals in the study area represent proxies for arid environment. Despite climate has interpreted through geomorphic landforms; mineralogical factors are mostly used as proxies to establish humid, semi-arid and arid palaeoclimatic investigations.

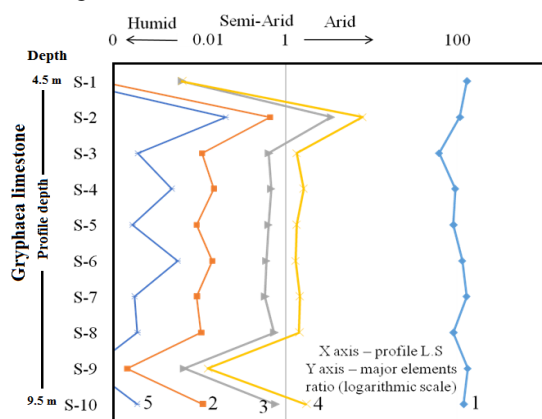


**Figure 10.** Ratio plot diagram of limestone samples of profile-I (average) plotted on the climate model diagram related to depth proposed by (after Smykatz-Kloss and Roy 2010; Udayanapillai et al., 2015). 1) CaO/MgO, 2) Na<sub>2</sub>O/Al<sub>2</sub>O<sub>3</sub>, 3) Na<sub>2</sub>O/K<sub>2</sub>O, 4) Na<sub>2</sub>O/TiO<sub>2</sub>, and 5)

Highly soluble major oxides Na<sub>2</sub>O, MgO, K<sub>2</sub>O, and un-soluble hydrolysate TiO<sub>2</sub>, Al<sub>2</sub>O<sub>3</sub> and Fe<sub>2</sub>O<sub>3</sub> are used as proxies to interpret the palaeoclimate studies of the Gryphaea limestone profile of the study area. The ratio of alkaline/hydrolysate is generally low in the humid climate and high in the arid climate (Sinha et al., 2006; Udayanapillai et al., 2021). Ratio value of Na<sub>2</sub>O/Al<sub>2</sub>O<sub>3</sub> (0.15), Na<sub>2</sub>O/Fe<sub>2</sub>O<sub>3</sub> (0.03), Na<sub>2</sub>O/K<sub>2</sub>O (0.88), Na<sub>2</sub>O/TiO<sub>2</sub> (1.8), and CaO/MgO (102.9) of the gryphaea limestone profile samples of the study area are given in (Table 4) and its ratio plot for climate model diagram related to depth are given in

the diagram (after Udayanapillai et al., 2015, 2021; Fig 10). The ratio value of < 0.1, 0.1 to 1, and >1 are treated as humid, semi-arid, and arid climates respectively, Geochemical ratio plots of gryphaea limestone samples collected from the study area fall on the semi-arid and arid climate prevailing during the depositional environment.

Aridity is established by Salinization. Salinization factor is established by the geochemical ratio of Na<sub>2</sub>O/K<sub>2</sub>O. When the above ratio is greater than 0.01, it represents a semi-arid and arid climate (Udayanapillai et al., 2015, 2021). The average Na<sub>2</sub>O/K<sub>2</sub>O ratio of the limestones is 0.88. This range in the profile represents the semi-aridity or aridity of the depositional environment. Calcification character is another factor in establishing palaeoclimate. It is established by the average geochemical ratio of CaO/MgO. Average calcification ratio of the gryphaea limestone profile is 102.93. Calcification is generally high in the study area which represents an arid environment.

Na<sub>2</sub>O/K<sub>2</sub>O, Na<sub>2</sub>O/Al<sub>2</sub>O<sub>3</sub>, and Na<sub>2</sub>O/TiO<sub>2</sub> ratios are high in an arid environment and vice versa in a humid environment in limestone deposits (Sinha et al., 2006; Udayanapillai et al., 2021). Similarly, high ratio values in limestones represent an arid and semi-arid climate conditions.

### CLAY MINERAL PROXIES

Limestone possesses regolith clay minerals and neo-formed clay minerals which represent climate history. Hydrolysis of weathered silicate minerals causes for the origin of clay. Meteoritic precipitation and the formation of clay minerals in the sediments help to interpret the palaeoclimate of sediments (Udayanapillai et al., 2015, 2022). Size, composition of parent material, temperature, seasonal rainfall, and time of formation of sediments are prime criteria for clay mineral composition (Udayanapillai et al., 2015, 2022). Some of the clay minerals represent the climate. Palygorskite and Sepiolite are indicating the arid climate. XRD analysis of gryphaea limestone shows the presence of clay minerals, such as kaolin, montmorillonite, and palygorskite which indicates arid and semi-arid climate conditions. Palygorskite is a neo-formed clay mineral in limestone formation that indicates an arid climate (Udayanapillai et al., 2015, 2022). Kaolin indicates a semi-arid climate (Udayanapillai et al., 2022). Gryphaea limestone of the study area represents semi-arid and arid climate conditions, during deposition.

### CONCLUSION

Pudupalayam Chettinadu limestone mine is located in the southern terminal part of the Kallankurichi formation of the Upper Cretaceous Ariyalur stage, Tamil Nadu, India. Petrological observation represents that the limestone does not

have mega fossils and generally a mud based biogenic limestone. However, it contains pelecypod, gastropod, shell fragments, microfossil groups of foraminifera, bryozoa, and algal mats. XRD result indicates the presence of many carbonate minerals and a few clay minerals. Geochemical results indicate elevated CaO concentration, due to the presence of more calcite minerals in the samples. Geostatistical analysis of multiple correlations, PCA, and Cluster analysis illustrates the geochemical affinities and inter-relationship between the geochemical elements. Palaeoclimate established through proxies of biota, geochemical ratio, and clay minerals indicate that the gryphaea limestone is formed under arid and semi-arid climates.

#### ACKNOWLEDGEMENTS

The First author expresses his sincere thanks to Shri. A.P.C.V. Chockalingam, Secretary and our Principal Dr. C. VeeraBhahu, V.O.Chidambaram College, Thoothukudi. The help was extended by Dr. P. Sivasubramanian, Professor and Head, PG and Research Department of Geology, V.O.Chidambaram College, Thoothukudi. John S. Armstrong-Altrin acknowledges the Sabbatical Research approved by PASPA, UNAM. This work is part of the PhD thesis of the first author M. Senthippan (Reg. no: 19212232221035).

#### ETHICS DECLARATIONS

#### CONFLICT OF INTEREST

The authors declare that they have no conflict of interest.

#### REFERENCE

- Anaya-Gregorio, A., Armstrong-Altrin, J.S., Machain-Castillo, M.L., Montiel-García, P.C., Ramos-Vázquez, M.A. (2018). Textural and geochemical characteristics of late Pleistocene to Holocene fine-grained deep-sea sediment cores (GM6 and GM7), recovered from southwestern Gulf of Mexico. *Journal of Palaeogeography*, 7(3), 253-271.
- Armstrong-Altrin, J.S. (2020). Detrital zircon U-Pb geochronology and geochemistry of the Riachuelos and Palma Sola beach sediments, Veracruz State, Gulf of Mexico: a new insight on palaeoenvironment. *Journal of Palaeogeography*, 9 (4), article no. 28.
- Armstrong-Altrin, J.S., Madhavaraju, J., Vega-Bautista, F., Ramos-Vázquez, M.A., Pérez-Alvarado, B.Y., Kasper-Zubillaga, J.J., EkoaBessa, A.Z. (2021b). Mineralogy and geochemistry of Tecolutla and Coatzacoalcos beach sediments, SW Gulf of Mexico. *Applied Geochemistry*. 134, 105103 <https://doi.org/10.1016/j.apgeochem.2021.105103>.
- Armstrong-Altrin, J.S., Ramos-Vázquez, M.A., Machain-Castillo, M.L., Márquez-García, A.Z. (2022). Geochemistry of marine sediments adjacent to the Los Tuxtlas Volcanic Complex, Gulf of Mexico: Constraints on weathering and provenance. *Applied Geochemistry*, 141, 105321. <http://doi.org/10.1016/j.apgeochem.2022.105321>.
- Armstrong-Altrin, J.S., Ramos-Vázquez, M.A., Zavala-León, A.C., Montiel-García, P.C. (2018). Provenance discrimination between Atasta and Alvarado beach sands, western Gulf of Mexico, Mexico: Constraints from detrital zircon chemistry and U-Pb geochronology. *Geological Journal*, 53(6), 2824-2848. <https://doi.org/10.1002/gj.3122>.
- Ayyasamy, K., Radhakrishnan, K., Lingaraj, Ota (1992). Stratigraphy of the Cretaceous rock around Kilapalavur, Trichirappalli district, Tamilnadu. *Palaeontological Society of India*, 109-112.
- Babu, K. (2017). Geochemical characteristics of sandstones from Cretaceous Garudamangalam area of Ariyalur, Tamilnadu, India: Implications of provenance and tectonic setting. *Journal of Earth System Science*, 126(4), 1.
- Banerji, R.K., Ramasamy, S., Malini, C.S., Singh, D. (1996). Uttatur group redefined. *Geological Society India, Memoirs*, 213-229.
- Blanford, H.F. (1862). On the Cretaceous and other rocks of South Arcot and Trichinopoly district. *Memoir Geological Survey of India*. 1-217.
- Botello, A.V., Ponce-Vélez, G., Armstrong-Altrin, J.S., Fragoso, S.V., Velandia-Aquino, L.B. (2023). Concentration of polycyclic aromatic hydrocarbons (PAHs) in sediments from the Tampamachoco lagoon, Tuxpan River mouth, Gulf of Mexico. *Arabian Journal of Geosciences*, 16, 556.
- Carroll, D. (1970). *Clay Minerals: A guide to their X-ray diffraction*. Geological Society of America Special Publication, 126:50. <https://doi.org/10.1130/SPE126-p1>
- Chougong, D.T., Bessa, A.Z.E., Ngueutchoua G., Yongue, R.F., Ntyam, S.C., Armstrong-Altrin, J.S. (2021). Mineralogy and geochemistry of Lobé River sediments, SW Cameroon: Implications for provenance and weathering. *Journal of African Earth Sciences*, 183, 1-19 No. 104320. <https://doi.org/10.1016/j.jafrearsci.2021.104320>.
- Clarke, A., Lidgard, S. (2000). Spatial patterns of diversity in the sea: bryozoan species richness in the North Atlantic. *Journal of Animal Ecology*, 69(5), 799-814.
- Cox, R., Lowe, D.R., Cullers, R.L. 1995. The influence of sediment recycling and basement composition on evolution of mud rock chemistry in the South-western United States. *Geochemical Cosmochimica Acta*, 59(14), 2919-2940.
- Davis, J.C. (1973). *Statistics and data analysis in geology*. John Wiley and Sons. New York, pp.

550.  
<https://doi.org/10.1180/minmag.1976.040.315.20>
- Deer, W.A., Howie, R.A., Zussman, J. (1979). An introduction to the rock-forming minerals. The English Language book Society and Longman, p 1–528.
- Dunham, R.J. (1962). Classification of carbonate rocks according to depositional textures.
- Ekoa Bessa, A.Z., Paul-Désiré, N., Fuh, G.C., Armstrong-Altrin, J.S., Betsi, T.B. (2021a). Mineralogy and geochemistry of the Ossa lake Complex sediments, Southern Cameroon: Implications for paleoweathering and provenance. *Arabian Journal of Geosciences*, 14, Article no. 322.
- Ekoa Bessa, A.Z., Armstrong-Altrin, J.S., Fuh, G.C., Betsi, T.B., Kelepile, T., Ndjigui, P-D. (2021b). Mineralogy and geochemistry of the Ngaoundaba Crater Lake sediments, northern Cameroon: implications for provenance and trace metals status. *Acta Geochimica*, 40, 718-738.
- Folk, R.L. (1968). Bimodal super mature sandstones: product of the desert floor. *Int. Geol. Congr.*, 23rd Sess., Proc., Sect. 8: 9--32.
- Goswami, A., Prasad, G.V.R., Verma, O., Flynn, J.J., Benson, R.B.J. (2013). A troodontid dinosaur from the latest Cretaceous of India (Abstract). *Nature communications* Art No: 1703, Doi 10.1038/ncomms 2716.
- Govindan, A., Ravindran, C.N., Rangaraju, M.K. (1996). Cretaceous stratigraphy and planktonic foraminiferal zonation of Cauveri Basin, South India. Sahni, A. (eds), In: *Cretaceous stratigraphy and palaeo-environments*. *Journal of Geological Society India*, 37, 155-187.
- Harper, D.A.T. (1999). *Numerical Palaeobiology*, John Wiley & Sons, New York. <https://doi.org/10.1017/S0016756800334410>
- Jiménez-Espinosa, R., Jiménez-Millán, J. (2003). Calcrete development in Mediterranean colluvial carbonate systems from SE Spain. *Journal of Arid Environments* 53(4), 479–489.
- Kaliammal, M., Udayanapillai, A.V. (2018). Aqueous geochemical modelling in the granite terrain of Pandalgudi aquifer region, Viruthunagar District, Tamilnadu, India. *IJCRT*, 6(2), 442-448.
- Kile, D.E., Dennis, E.D. (2000). Quantitative mineralogy and particle-size distribution of Bed Sediments in the Boulder Creek Watershed. *Mineralogy and Particle-size of Bed Sediments*, pp. 173–184
- Krishnan, M.S. (1982). *Geology of India and Burma*, CBS publishers and distributor (eds), 536p
- Kuttalingam, U., Udayanapillai, A.V., Murugan, D., Lakshmanan, C. (2018). Advanced computational geostatistical studies of groundwater quality of Vilathikulam Region, Thoothukudi District, Tamilnadu, India. *International Journal of Recent Research Aspects* 20,1024-1029.
- Madhavaraju, J., Ramasamy, S. (1999). Rare earth elements in limestones of Kallankurichchi Formation of Ariyalur Group, Tiruchirapalli Cretaceous, Tamil Nadu., *Journal of the Geological Society of India*, 54, 291-301.
- Madhavaraju, J., Armstrong-Altrin, J.S., Pillai, R.B., Pi-Puig, T. (2021). Geochemistry of sands from the Huatabampo and Altata beaches. *Gulf of California, Mexico. Geological Journal*, 56, 2398-2417. DOI:10.1002/gj.3864.
- Mitra, S. (1989). *Fundamental of optical spectroscopic and X-ray. Mineralogy* Wiley. <http://www.worldcat.org/oclc/17300449>
- Nagendra, R., Kannan, B.K., Sen, G., Gilbert, H., Bakkiaraj, D., Reddy, A.N., Jaiprakash, B.C. (2018). Sequence surfaces and paleobathymetric trends in Albion to Maastrichtian sediments of Ariyalur area, Cauvery Basin, India. *Marine and Petroleum Geology*, 28(4), 895-905.
- Nagendra, R., Nagarajan, R., Bakkiaraj, D., Armstrong-Altrin, J.S. (2011). Depositional and post-depositional setting of Maastrichtian limestone, Ariyalur Group, Cauvery Basin, South India: a geochemical appraisal. *Carbonates and Evaporites*, 26(2), 127-147.
- Nagendra, R., Nagendran, G., Narasimha, K., Jaiprakash, B.C., Nallapa Reddy, A. (2002). Sequence stratigraphy of Dalmiapuram formation Kallakudi Quarry – II, South India, *Journal of Geological Society of India*, 59, 249-258.
- Nagendra, R., Sathiyamoorthy, P., Pattanayak, S., Nallapa Reddy, A., Jaiprakash, B.C. (2013). Stratigraphy and paleobathymetric interpretation of the Cretaceous Karai shale formation of Uttatur Group, TamilNadu, India. *Stratigraphy and Geological Correlation*, 21, 675-688.
- Nagendra, R., Nallapa Reddy, A. (2017). Major geologic events of the Cauvery Basin, India and their correlation with global signatures- A review. *Journal of Palaeogeography*, 6(1), 69-83
- Nagendra, R., Nallapa Reddy, A. (2017). Major geologic events of the Cauvery Basin, India and their correlation with global signatures- A review. *Journal of Palaeogeography*, (1), 69-83.
- Nagendra, R., Reddy, A.N., Jaiprakash, B.C., Gilbert, H., Zakharov, Y.D., Venkateshwarlu, M. (2018). Integrated Cretaceous stratigraphy of the Cauvery basin, south India. *Stratigraphy*, 15(4), 245-249.
- Perumal, V., Udayanapillai, A.V. (2020). Calcrete profiles in Puthukulam quarry section, Sathankulam region, Southern Tamilnadu, India, implications on palaeoclimate significance. *Journal of Sedimentary Environment* 5:493503.
- Praus, P. (2007). Urban water quality evaluation using multivariate analysis. *Acta Montan. Slovaca* 12(2):50–158.

- Ramasamy, S., Banerji, R.K. (1991). Geology, Petrography and Stratigraphy of Pre-Ariyalur sequence in Trichirapalli district, Tamilnadu. *Journal of the Geological Society of India*, 577-594.
- Ramasamy, S., Ramachandran, A., Velmurugan, K., David Lalhmimgliana Chawngthu, B.S., Suresh Gandhi, M. (2012). Sedimentological studies of Kallamedu Formation in Ariyalur area, Tamil Nadu, India. *International Journal of Geology, Earth and Environmental Sciences*, 2, 218-234.
- Ramasamy, S., Singh, T.S., Madhavaraju, J., Asir, G.G. (2007). Petrography and geochemistry of pre-Ariyalur sequence in Perambalur District, Tamil Nadu-Implications on depositional environment and palaeoclimate. *Journal of the Geological Society of India*, 69(1), 121-132.
- Ramkumar, M.U. (2008). Carbonate Diagnosis in the Kallankurichchi Formation, Ariyalur Group, South India and its Implications on Petroleum Prospects. *Journal of the Geological Society of India*, 71(3), 407.
- Ramkumar, K.B., Rajkumar, P.K., Ahmmad, S.N., Jegan, M. (2020). A review on performance of self-compacting concrete—use of mineral admixtures and steel fibres with artificial neural network application. *Construction and Building Materials*, 261, 120215.
- Ramos-Vázquez, M.A., Armstrong-Altrin, J.S. (2019). Sediment chemistry and detrital zircon record in the Bosque and Paseo del Mar coastal areas from the southwestern Gulf of Mexico. *Marine and Petroleum Geology*, 110, 650-675.
- Ramos-Vázquez M.A., Armstrong-Altrin J.S. (2021) Provenance of sediments from Barra del Tordo and Tesoro beaches, Tamaulipas State, north-western Gulf of Mexico. *Journal of Palaeogeography*, 10(1).
- Ramos-Vázquez, M.A., Armstrong-Altrin, J.S., Madhavaraju, J., Gracia, A., Salas-de-León, D.A. (2022). Mineralogy and geochemistry of marine sediments in the Northeastern Gulf of Mexico. In: Armstrong-Altrin JA, Pandarinath K, Verma S. (Eds.), *Geochemical Treasures and Petrogenetic Processes*. P. 153-183 [https://doi.org/10.1007/978-981-19-4782-7\\_7](https://doi.org/10.1007/978-981-19-4782-7_7)
- Reddy, A.N., Jaiprakash, B.C., Rao, M.V., Chidambaram, L., Bhaktavatsala, K.V. (2013). Sequence stratigraphy of late Cretaceous successions in the Ramnad sub-basin, Cauvery Basin, India. In *Proc. XXIII Indian Colloquium on Micropaleontology and Stratigraphy and International Symposium on Global Bioevents in Earth History*. Geological Society of India Special Publications, No. 1, pp. 78-97.
- Shrock, Twenhofel (2005). *Principles of Invertebrate Palaeontology*, Second edition, CBS, pp 1-816.
- Sinha, R., Smykatz-Kloss, W., Stüben, D., Harrison, S. P., Berner, Z., Kramar, U. (2006). Late Quaternary palaeoclimatic reconstruction from the lacustrine sediments of the Sambhar playa core, Thar Desert margin, India. *Palaeogeography, Palaeoclimatology, Palaeoecology*, 233(3-4), 252-270.
- Smykatz-Kloss, W., Roy, P.D. (2010). Evaporite mineralogy and major element geochemistry as tools for palaeoclimatic investigations in arid regions: A synthesis. *Boletín de la Sociedad Geológica Mexicana*, 62(3), 379-390.
- Sopie, F.T., Ngueutchoua, G., Armstrong-Altrin, J.S., Njanko, T., Sonfack, A.N., Sonfack, A.N., Ngagoum, Y.S.K., Fossa, D., Tembu, L.T. (2023). Provenance, weathering, and tectonic setting of the Yoyo, Kribi, and Campo beach sediments in the southern Gulf of Guinea, SW Cameroon. *Journal of Earth System Science* <https://doi.org/10.1007/s12040-023-02101-5>
- Sridhar, M., Chaturved, A., Rai, A., (2014). Locating new uranium occurrence by integrated weighted analysis in Kaladgi basin, Karnataka. *Journal of the Geological Society of India*, 84(5), 509–512. <https://doi.org/10.1007/s12594-014-0159-2>
- Srinivasamoorthy, K., Vijayaraghavan, M., Vasanthavigar, V.S., Sarma, S., Chidambaram, P., Anandhan (2010). Assessment of groundwater quality with special emphasis on fluoride contamination in crystalline bed rock aquifers of Mettur region, Tamilnadu, India. *Arabian Journal of Geosciences*, 5, 83–94. <https://doi.org/10.1007/s12517-010-0162-x>
- Srivastava, P., Parkash, B., Pal, D.K. (1998). Clay minerals in soils as evidence of Holocene climatic change, Central Indo-Gangetic Plains, North-Central India. *Quaternary Research*, 50(3), 230–239
- Sundaram, R., Henderson, R.A., Ayyasami, K., Stilwell, J.D. (2001). A lithostratigraphic revision and palaeo-environmental assessment of the Cretaceous system exposed in the onshore Cauvery Basin, southern India. *Cretaceous Research*, 22, 743-762.
- Tawfik, H.A., Salah, M.K., Maejima, W., Armstrong-Altrin, J.S., Abdel-Hameed, A-M.T., Ghandour M.M.E. (2018). Petrography and geochemistry of the Lower Miocene Moghra sandstones, Qattara Depression, north Western Desert, Egypt. *Geological Journal*, 53, 1938-1953.
- Udayanapillai A, V., Velmayil, P., Armstrong-Altrin, J.S. (2020). Provenance, Weathering, Tectonic setting and Palaeo-oxygenation condition of the Cretaceous Calcareous Grey Shale (CGS) from the Kallakudi Dalmia Limestone Quarry No:II, Uttatur group, Trichinopoly, Tamilnadu, India. *Himalayan Geology*, 41(1), 11-2.
- Udayanapillai, A.V., Perumal, V., Thirugnasambandam, R., Venkataraman, P., Thangavel, M. (2015). Study of micro-morphology, major element geochemistry and palaeoclimatic implications of calcrete deposits at Salukkuvarpatti Village, Near Pandalgudi, Viruthunagar District, Tamilnadu, India. *Journal of Applied Geochemistry*, 17(4), 421-43.

- Udayanapillai, A.V., Velmayil, P., Armstrong-Altrin, J.S., Sial, A., Manavalan, S. (2022). Geochemical and stable isotope ( $\delta^{13}\text{C}$  &  $\delta^{18}\text{O}$ ) signatures of calcrete in and around Pandalgudi, Southern Tamilnadu, India and its implications on Palaeoclimate, *Arabian Journal of Geosciences*, 15(913), 1-19. <https://doi.org/10.1007/s12517-022-10134-1>.
- Udayanapillai, A.V., Velmayil, P. (2021). Texture, mineralogy and geochemistry of Teri sediments from the Kuthiraimozhi deposit, Southern Tamilnadu, India: implications on provenance, weathering and palaeoclimate. *Arabian Journal of Geosciences*, 14(5), 1-15.
- Udayanapillai A.V., Kaliasammal, M. (2016). Groundwater Characterization and Quality Assessment by using GIS and Geo Statistics from Pandalgudi Region, Virudhunagar District, Tamilnadu, India. *International Journal of Research in Environmental Science (IJRES)* Volume 2, Issue 4, PP 1-16 ISSN 2454-9444 <http://dx.doi.org/10.20431/2454-9444.0204001>.
- Udayanapillai, A.V., Ganesamoorthy (2013). Mineralogy and Geochemistry of Red and Black sediments of Thoothukudi District, Tamilnadu, India. *Journal Geological Society Sri Lanka*, 15, pp. 47-56
- Usman, M.O., Masago, H., Winkler, W., Strasser, M. (2014). Mid-Quaternary decoupling of sediment routing in the Nankai Forearc revealed by provenance analysis of turbiditic sands. *International Journal of Earth Sciences*, 103, 1141-1161.
- Wright, J.L., Unwin, D.M., Lockleyl, M.G., Rainforth, E.C. (1997). Pterosaur tracks from the Purbeck limestone Formation of Dorset, England. *Proceedings of the Geologists' Association*, 108(1), 39-48.